JOURNAL OF MATERIALS SCIENCE 10 (1975) 214–222

The fracture stress and its dependence on slow crack growth

A. G. EVANS*, H. JOHNSON
Inorganic Materials Division, Institute of Materials Science, National Bureau of Standards, Washington, D.C., USA

An analysis is presented which enables the fracture strength, (under constant stress-rate conditions) to be predicted from fracture mechanics data obtained during slow crack growth – by identifying and evaluating several key parameters. The predicted strength characteristics are illustrated using fracture mechanics data obtained for a soda lime silicate glass. Finally, the predicted strengths are compared with strengths measured in flexure on abraded soda lime silicate glass specimens. A good correlation is obtained, indicating an equivalence between micro- and macro-crack propagation conditions for this material.

1. Introduction

When slow crack growth occurs, the extent of the slow crack growth affects the fracture stress. This problem was first examined by Charles [1], for constant stress-rate conditions, by assuming a single functional relation to describe the slow crack growth. More recently, Evans [2] has approached the problem from first principles, commencing with the fundamental fracture mechanics characterization of slow crack growth (which relates the crack growth rate, V, to the stress intensity factor, K_I). A typical slow crack growth behaviour [3], illustrated in Fig. 1, exhibits four regions. A region of zero slow crack growth below K_0; a variable velocity region, I, between K_0 and K_{Ib}; a constant velocity (V_b) region, II; and another region of variable velocity, III, prior to the onset of rapid fracture at K_{IC}. Each region can be characterized by the relation

$$V = \frac{da}{dt} = AK_I^n \qquad (1)$$

where a is the crack length and A and n are constant for *each region*; e.g. in region I, n is typically in the range 10 to 70 [4]; in region II, n is ~ 0 [3]; and in region III n is very large ($\gtrsim 50$) [5, 6]. Starting with Equation 1 Evans [2] demonstrated that, for constant stress-rate conditions, the fracture stress should display the general features shown in Fig. 2: a region B that corresponds to region I of the K_I, V diagram and region B′ and C that relate respectively to regions II and III. The same basic fracture stress characteristics were also demonstrated [2] to exist for the more generally used constant strain-rate conditions, except for situations where the initial crack size was a significant fraction of the specimen thickness. This situation is rarely

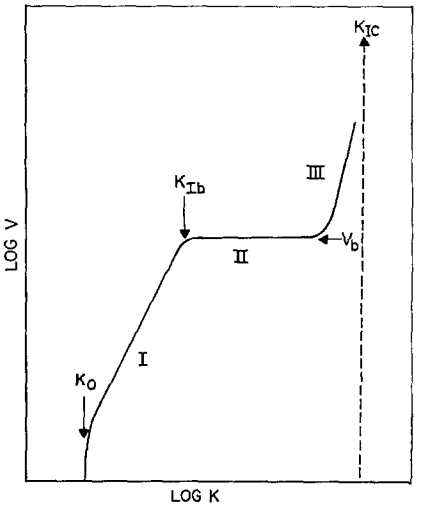

Figure 1 A schematic of a typical three stage slow crack growth diagram.

*Present address: Science Center, Rockwell International, Thousand Oaks, California 91360, USA

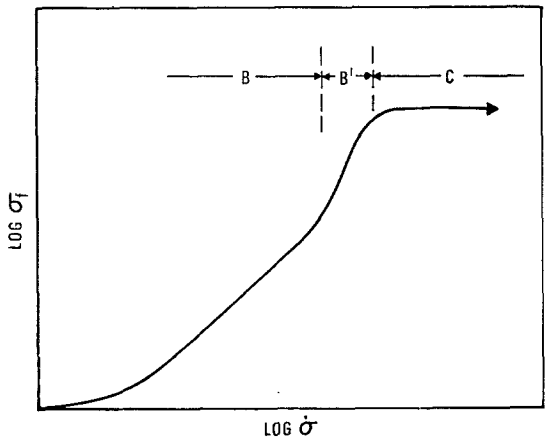

Figure 2 A schematic of the stress-rate dependence of the strength, predicted from the three stage crack growth behaviour depicted in Fig. 1.

encountered in ceramic systems and hence, the constant stress-rate analysis of crack growth can generally be used to predict the fracture stress.

Commencing with this basic knowledge, we intend in this paper to develop analyses which predict *in detail* the relations between fracture stress σ_f and the stress rate $\dot{\sigma}$ from K_I, V diagrams; and to present the results in a form that will permit the reader to develop σ_f, $\dot{\sigma}$ diagrams from K_I, V diagrams *for any system*, by performing a few very simple calculations.*

The analysis is followed by a comprehensive empirical evaluation of the fracture stress, stress-rate relation for a soda lime glass under controlled environmental conditions. Finally, the measured σ_f, $\dot{\sigma}$ diagram is compared with the diagram predicted from existing K_I, V data [3].

2. Slow crack growth during loading – analysis

2.1. The crack growth relation

The extent of the slow crack growth that occurs in ceramic materials under *any* imposed loading condition can be determined from Equation 1, by combining with the fracture mechanics relation, $K_I = \sigma Y\sqrt{a}$ (where σ is the stress and Y is a geometric constant), and separating the variables, to give

$$\frac{da}{a^{n/2}} = A Y^n \sigma^n dt . \tag{2}$$

For a constant stress rate, $\dot{\sigma}$, the stress is given by

$$\frac{\sigma - \sigma_i}{t - t_i} = \dot{\sigma} \tag{3}$$

where σ_i and t_i are the stress and time at the initial condition. Differentiating Equation 3 and substituting in Equation 2 gives

$$\frac{da}{a^{n/2}} = \frac{A Y^n \sigma^n d\sigma}{\dot{\sigma}} \tag{4}$$

This may be integrated to give

$$\frac{1}{a_i^{(n-2)/2}} - \frac{1}{a^{(n-2)/2}} = \frac{(n-2)A Y^n}{(n+1)2\dot{\sigma}} (\sigma^{n+1} - \sigma_i^{n+1}) \tag{5}$$

where a_i is the initial crack length. This is the *fundamental* relation used for the prediction of failure under constant stress-rate conditions.

The failure condition can be derived from Equation 5 in several ways, but we find that an appreciation of the problem is most effectively achieved by establishing the relation between the stress and the stress intensity factor during the loading process. A convenient intermediary step in the development of the σ, K_I diagram is the evaluation of the crack length, stress intensity factor relation, which is obtained in general form from Equation 5, by substituting for the stress ($\sigma = K/Y\sqrt{a}$), to give

$$a^{3/2}\left\{\left(\frac{a}{a_i}\right)\frac{n-2}{2}\left[1 + \left(\frac{n-2}{n+1}\right)\frac{A}{2Y\dot{\sigma}} K_{Ii}^{n+1} a_i^{-3/2}\right] - 1\right\} = \left(\frac{n-2}{n+1}\right)\frac{A}{2\dot{\sigma} Y} K_I^{n+1} . \tag{6}$$

2.2. The crack propagation stress

2.2.1. Region I

For initial propagation, the initial stress intensity factor, K_{Ii}, is zero (assuming no slow crack growth limit) and region I slow crack growth determines the crack propagation condition; hence, from Equation 6,

$$a^{3/2}\left[\left(\frac{a}{a_i}\right)^{(n_1-2)/2} - 1\right] = \left(\frac{n_1-2}{n_1+1}\right)\frac{A_1}{2\dot{\sigma} Y} K_I^{n_1+1} \tag{7}$$

*The σ_f, $\dot{\sigma}$ predictions from K_I, V diagrams are only expected to give a strict representation of the strength when the macro fracture mechanics behaviour simulates the slow crack growth at the small pre-existing flaws.

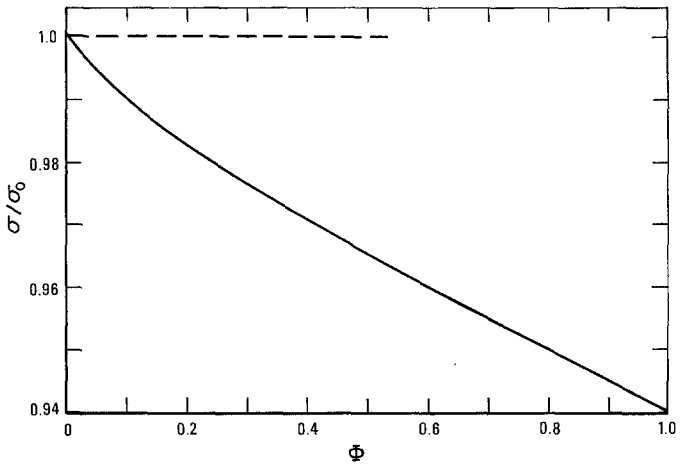

Figure 3 The effect of Φ at constant K_I on the stress ratio σ/σ_0, due to region I slow crack growth.

where the subscript 1 refers to region I behaviour. This equation can be solved for small or large crack extensions.

(a) For small crack extensions, rewriting Equation 7 as

$$a_i^{3/2}\left[1+\frac{\Delta a}{a_i}\right]^{3/2}\left[\left(\frac{\Delta a}{a_i}+1\right)^{(n-2)/2}-1\right] = \frac{A_1 K_I^{n_1+1}}{2Y\dot{\sigma}}\left(\frac{n_1-2}{n_1+1}\right) \quad (8)$$

where $\Delta a = a - a_i$, we obtain

$$\frac{(n_1+2)}{4}\left(\frac{\Delta a}{a_i}\right)^2+\left(\frac{\Delta a}{a_i}\right) - \frac{K_I^{n_1+1}A_1}{Y(n_1+1)\dot{\sigma}a_i^{3/2}}=0 \quad (9)$$

which can be solved to give

$$\frac{\Delta a}{a_i} = \frac{2}{(n_1+2)}\left\{\left[1+\frac{(n_1+2)A_1K_I^{n_1+1}}{Y\dot{\sigma}(n_1+1)a_i^{3/2}}\right]^{1/2}-1\right\} \equiv \frac{2}{(n_1+2)}\left[(1+\Phi)^{1/2}-1\right]. \quad (10)$$

Substituting the stress for the crack length ($a = K_I^2/Y^2\sigma^2$) then gives the stress during initial propagation, and its dependence on K_I;

$$\sigma = \sigma_0(n_1+2)^{1/2}[n_1+2(1+\Phi)^{1/2}]^{-1/2} \quad (11)$$

where $\sigma_0 (= K_I Y\sqrt{a_i})$ is the stress that would be attained at the equivalent K_I when no slow crack growth occurs. It is apparent from Equation 11 that the crack propagation stress σ does not deviate very rapidly from σ_0 during initial propagation, unless n is very small. This feature is illustrated in Fig. 3 by taking the smallest known n value for ceramic materials, i.e. 10 (for silicon nitride [4]), and plotting σ/σ_0 versus Φ. We have found it useful for plotting the σ, K_I diagram to *define* a stress, σ^*, as the stress where σ first deviates significantly from σ_0, (say, $\sigma^* = 0.99\ \sigma_0$). This stress is obtained directly from Equation 11 and the definition of σ_0, to give

$$\sigma^* = \frac{0.99}{Y\sqrt{a_i}}\left\{\frac{Y\dot{\sigma}a_i^{3/2}}{4A_1}\left(\frac{n_1+1}{n_1+2}\right)\left[\frac{0.16+0.04n_1+(0.02n_1)^2}{0.96}\right]\right\}^{1/(n_1+1)}. \quad (12)$$

(b) For larger crack extensions, since n_1 is generally a large number, the quantity $(a/a_i)^{(n_1-2)/2}$ very rapidly becomes much larger than unity; then Equation 7 reduces to

$$a^{(n_1+1)/2} = \left(\frac{n_1-2}{n_1+1}\right)\frac{A_1}{2\dot{\sigma}Y}K_I^{n_1+1}\,a_i^{(n_1-2)/2} \quad (13)$$

Substituting the stress for the crack length we obtain

$$\sigma^{n_1+1} = \frac{2\dot{\sigma}(n_1+1)}{A_1 Y^{n_1}(n_1-2)a_i^{(n_1-2)/2}} \equiv \sigma_{max}{}^{n_1+1}. \quad (14)$$

Thus, the crack propagation stress must quickly assume a maximum, constant value, σ_{max} [1, 2]. For the development of σ, K_I diagrams we find that it is instructive to identify a condition where the stress essentially merges with the maximum stress asymptote given by Equation 14. Hence, we shall define a stress intensity factor, $K_I{}^*$, as the K_I value when the stress reaches $0.99\ \sigma_{max}$. The magnitude of $K_I{}^*$ is determined by first expres-

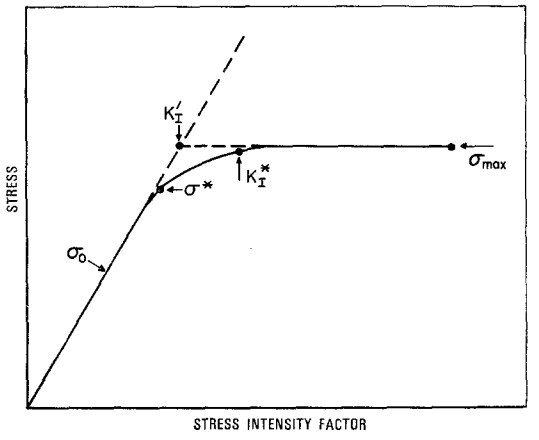

Figure 4 A schematic of the variation of stress intensity factor with stress for region I slow crack growth, defining the parameters: σ_0, σ^*, σ_{max}, K_I^* and K_I'.

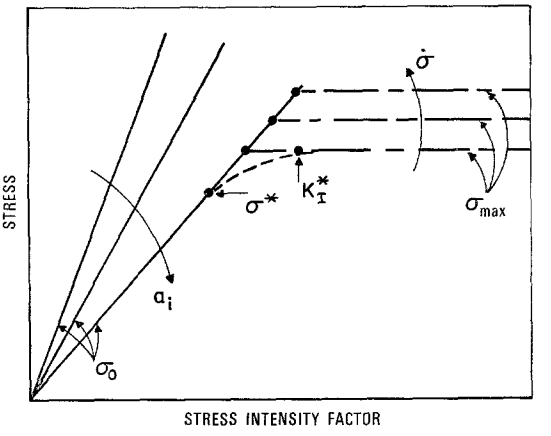

Figure 5 A schematic of the effect of a_i on σ_0 (independent of $\dot{\sigma}$) and the effect of $\dot{\sigma}$ on σ_{max} (at constant a_i), for region I slow crack growth.

sing Equation 7 in terms of stress and crack length (using $K_I = \sigma Y\sqrt{a}$) and then substituting for the specified stress (i.e. 0.99 σ_{max}) from Equation 14, to find the crack length a^* at K_I^*; this procedure yields

$$\frac{a^*}{a_i} = [1 - 0.99^{n_1+1}]^{-2/(n_1-2)} . \quad (15)$$

Substituting this value for a^* in Equation 7 then gives the desired result;

$$K_I^* = \frac{0.99\sigma_{max} Y\sqrt{a_i}}{[1 - 0.99^{n_1+1}]^{1/(n_1-2)}} . \quad (16)$$

The principal features of the crack propagation behaviour, expressed in terms of the σ, K_I diagram, can now be quite simply developed from the four parameters, σ_0, σ_{max}, σ^* and K_I^*, identified in Fig. 4. It is convenient to start with the stress $\sigma_0 (= K/Y\sqrt{a_i})$ which emerges as a series of straight lines with a functional dependence on a_i, as shown schematically in Fig. 5. Next, σ_{max} can be determined from Equation 14 for each a_i, and a corresponding range of stress rates (Fig. 5). Finally, σ^* and K_I^* may be obtained from Equations 12 and 16 and the complete curves drawn by connecting σ^* to K_I^*. This latter procedure is facilitated by noting that

$$\sigma^* = 0.99\sigma_{max}\left[\left(\frac{n_1 - 2}{n_1 + 2}\right)\left(\frac{0.16 + 0.04n_1 + (0.02n_1)^2}{7.68}\right)\right]^{1/(n_1+1)} \quad (17)$$

and that,

$$K_I^* = 0.99\, K_I'[1 - 0.99^{n_1+1}]^{-1/(n_1-2)} \quad (18)$$

where K_I' is the K_I value where σ_0 and σ_{max} intersect (Fig. 4). For typical n values for ceramic systems ($\lesssim$ 10) [4], we find that the ratios σ^*/σ_{max} and K_I^*/K_I' do not differ substantially from unity; also note that both ratios are *independent of* $\dot{\sigma}$ *and* a_i. For soda lime glass, for example, n is 16 [3, 7] so that σ^*/σ_{max} is 0.88 and K_I^*/K_I' is 1.13. Hence, the connection of σ^* to K_I^* essentially requires only a modest rounding of the curve near the intersection of σ_0 and σ_{max} and this can usually be performed manually without additional calculation, as shown by the dotted line in Fig. 5.

2.2.2. Region II

In region II, crack growth occurs essentially at constant velocity ($n = 0$) and Equation 5 becomes;

$$a - a_b = \frac{V_b}{\dot{\sigma}}(\sigma - \sigma_b) \quad (19)$$

where the subscript b refers to the magnitude of the parameters at the onset of region II. Substituting the stress intensity factor for the crack length (using, $K_I = \sigma Y\sqrt{a}$) and rearranging gives;

$$\left(\frac{\sigma}{\sigma_b}\right)^3 - \left(\frac{\sigma}{\sigma_b}\right)^2\left[1 - \left(\frac{K_{Ib}^2}{\sigma_b^3}\right)\left(\frac{\dot{\sigma}}{Y^2V_b}\right)\right] - \left(\frac{K_I^2}{\sigma_b^3}\right)\left(\frac{\dot{\sigma}}{Y^2V_b}\right) = 0 . \quad (20)$$

This equation can be solved for (σ/σ_b) using the standard cubic solution; but this is a tedious task and instead of presenting the detailed solution we believe that it is more useful to

identify the important characteristics of the equation.

The principal feature to note is that (σ/σ_b) only differs significantly from unity when the quantity $(K_I^2/\sigma_b^3)\ .\ (\dot{\sigma}/Y^2V_b)$ is larger than ~ 0.01. An important calculation to perform, therefore, is the evaluation of the quantity, $\xi = (K_{IP}^2/\sigma_b^3)\ .\ (\dot{\sigma}/Y^2V_b)$, where K_{IP} is the stress intensity factor at the end of region II. Let us evaluate the magnitude of ξ when σ is marginally larger than σ_b, say, 0.99σ: then, to facilitate the fracture stress determination we can define a critical stress-rate, σ_c, as the stress-rate when region II crack propagation first generates a significant increase in the crack propagation stress. Inserting $\sigma_b/\sigma = 0.99$ in Equation 20 gives

$$\xi = 10^{-2}[1 - (K_{Ib}/K_{IP})^2]^{-1} \tag{21}$$

and hence, from the definition of ξ we obtain

$$\dot{\sigma}_c = 10^{-2}\frac{Y^2V_b\sigma_b^3}{K_{IP}^2 - K_{Ib}^2}\cdot \tag{22}$$

Additionally, as noted in the analysis of region I behaviour, the crack propagation stress for $K_I < K_{Ib}$ very rapidly reaches the constant value, $(\sigma_{max})_1$, given by Equation 14. We can thus equate σ_b to $(\sigma_{max})_1$ without introducing any significant inaccuracies; hence,

$$\dot{\sigma}_c = \frac{1}{Ya_i^{3/2}}\left[\frac{10^{-2}V_b}{K_{IP}^2 - K_{Ib}^2}\right]^{(n_1+1)/(n_1-2)} \left[\frac{2}{A}\left(\frac{n_1+1}{n_1-2}\right)\right]^{3/(n_1-2)}\cdot \tag{23}$$

We are now in a position to formulate several important conclusions concerning the role of region II crack propagation. There is a critical stress-rate, $\dot{\sigma}_c$ given by Equation 23, below which the crack propagation stress in region II is essentially identical to that at the end of region I and determined exclusively by the region I crack propagation parameters. At stress-rates larger than $\dot{\sigma}_c$ a significant stress increase does occur in region II and its magnitude can be determined by solving Equation 20. Finally, it is noted that the critical stress-rate $\dot{\sigma}_c$ is not only a function of the regions I and II crack propagation parameters, but also is strongly dependent on the initial flaw size a_i: specifically, an *increase* in a_i by, say 10^2, *reduces* $\dot{\sigma}_c$, by 10^3.

2.2.3. Region III

For region III, the functional relation that describes the slow crack growth is similar to that for region I, although n is substantially larger (> 50). The analysis is then similar to the region I analysis, with the additional feature that the initial stress intensity factor is larger than zero. We shall denote this initial stress intensity factor by K_{IP} (i.e. the stress intensity factor at the end of region II), and insert this for K_{Ii} in Equation 6 to find the maximum crack propagation stress (using essentially the same procedure described for region I crack propagation). This procedure gives

$$(\sigma_{max})_3 = \sigma_P\left[1 + 2\left(\frac{\dot{\sigma}}{V_bY^2}\right)\left(\frac{K_{IP}^2}{\sigma_P^3}\right)\right]^{1/(n_3+1)} \equiv \sigma_P\left[1 + 2\xi\left(\frac{\sigma_b}{\sigma_P}\right)^3\right]^{1/(n_3+1)} \tag{24}$$

where the subscript 3 refers to region III behaviour and σ_P is the stress at the end of region II. Again, therefore, a significant stress increase in region III only occurs when ξ becomes a significant fraction of unity: since n_3 is a large number, we find that typically ξ must exceed ~ 0.2 to enable $(\sigma_{max})_3$ to significantly exceed σ_P. Hence, we conclude that no stress increase occurs in region III until a stress-rate is attained somewhat larger than the stress-rate needed to achieve a region II stress increase; this feature is illustrated schematically in Fig. 7.

When the stress-rate is sufficiently large, it is apparent from the trends depicted in Figs. 6 and 7 that significant crack propagation in regions I and II can be suppressed, such that $\sigma_P \approx \sigma_0$. In this stress-rate range the crack propagation can be treated in a manner equivalent to that described in region I; hence comparison with Equation 14 shows that the crack propagation stress rapidly assumes a constant maximum value, given by

$$(\sigma_{max})_3 = \left[\frac{2\dot{\sigma}K_{IP}^{n_3}}{Y^{n_3}V_b}\left(\frac{n_3+1}{n_3-2}\right)a_i^{(n_3-2)/2}\right]^{1/(n_3+1)}\cdot \tag{25}$$

We shall now define a critical stress-rate, $\dot{\sigma}_s$, as the stress-rate, above which Equation 25 completely describes the crack propagation stress. This stress-rate is obtained by putting $\sigma_P \approx \sigma_0$ (say, $\sigma_P = 0.99\sigma_0$). Commencing with Equation 20 and rewriting it in terms of crack lengths, we obtain

$$\left(\frac{a_P}{a_i}\right)^{3/2} + \left(\frac{a_P}{a_i}\right)^{1/2}\left[\frac{V_bK_{Ib}}{\dot{\sigma}Ya_i^{3/2}} - 1\right] - \frac{K_{IP}V_b}{\dot{\sigma}Ya_i^{3/2}} = 0\,. \tag{26}$$

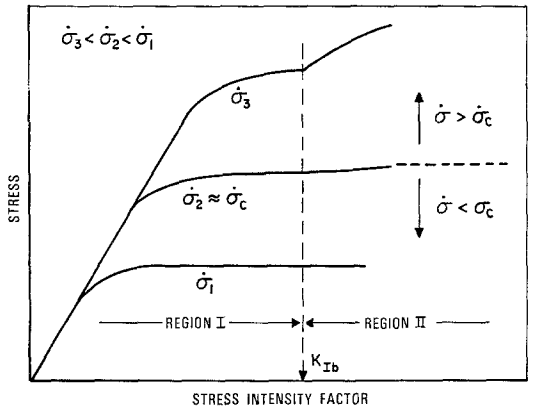

Figure 6 A schematic of the effect of stress-rate on the crack propagation stress, due to region II slow crack growth.

Substituting $a_P/a_i = 1.02$ (the crack length equivalent of $\sigma_P = 0.99\sigma_0$) and solving for $\dot{\sigma}$ then gives;

$$\dot{\sigma}_s = \frac{V_b(K_{IP} - K_{Ib})}{10^{-2} Y a_i^{3/2}} . \quad (27)$$

Note that the crack length dependence of $\dot{\sigma}_s$ is identical to that for $\dot{\sigma}_c$ (Equation 23). Hence, the extent of the stress-rate *range*, $\dot{\sigma}_c$ to $\dot{\sigma}_s$, where the crack propagation stress changes from completely region I dominated behaviour (below $\dot{\sigma}_c$) to completely region III dominated behaviour (above $\dot{\sigma}_s$), is independent of the initial flaw size. (The specific stress-rate *location* of this range is, of course, strongly dependent on a_i.)

2.3. The fracture stress

The fracture stress for constant stress-rate conditions is determined by the stress when the crack emerges from the specimen [2]. For small initial crack sizes (compared to the specimen thickness), K_I will be well into region III before the crack emerges from the specimen, at least for the stress-rates of practical interest. Hence, we may generally equate the maximum region III stress, $(\sigma_{max})_3$, to the fracture stress, σ_f. The fracture stress may thus be obtained in terms of the initial crack length and the stress-rate by combining Equations 21, 20 and 7. This procedure does not yield a simple analytical relation and it is more convenient to obtain a solution using the stepwise procedure described in the preceding section (considering each stage separately). This is illustrated by examining a specific example: soda lime glass in a 1% RH environment and an initial flaw size 10^{-5} m. The K_I, V data obtained by Wiederhorn [3] (Fig. 8) are used to compute the σ, K_I diagrams.

Initially, it is useful to evaluate the critical stress-rates $\dot{\sigma}_c$ and $\dot{\sigma}_s$. From Equation 23, $\dot{\sigma}_c$ is 4×10^{-1} MN m^{-2} sec^{-1} and, from Equation 27, $\dot{\sigma}_s$ is 10^3 MN m^{-2} sec^{-1}. Next, to obtain the fracture stress at stress-rates below $\dot{\sigma}_c$ we can simply equate σ_f to $(\sigma_{max})_1$, giving $\sigma_f \propto \dot{\sigma}^{1/(n_1+1)}$

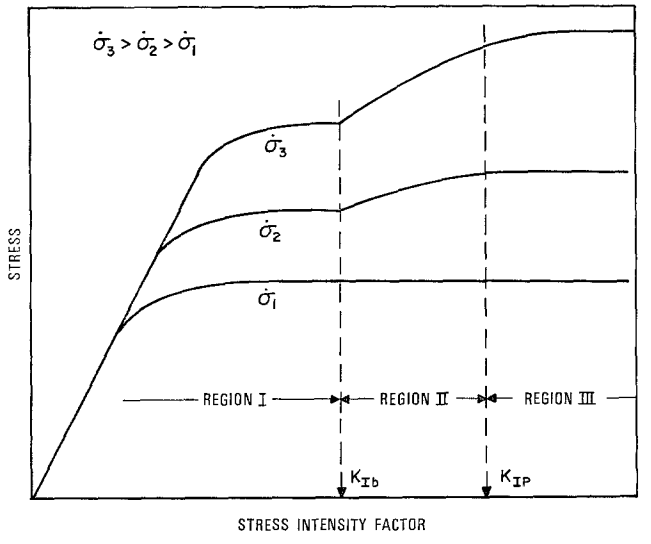

Figure 7 A schematic of the effect of stress-rate on the crack propagation stress, due to region III slow crack growth.

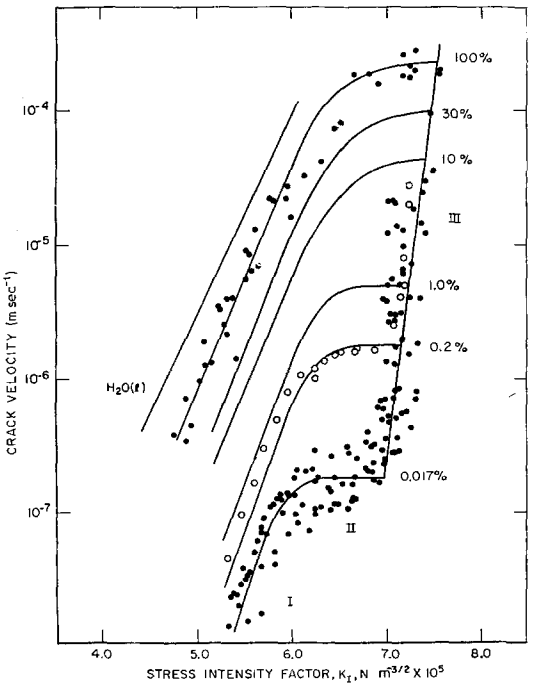

Figure 8 Slow crack growth data for soda lime glass as a function of the relative humidity (after [3]).

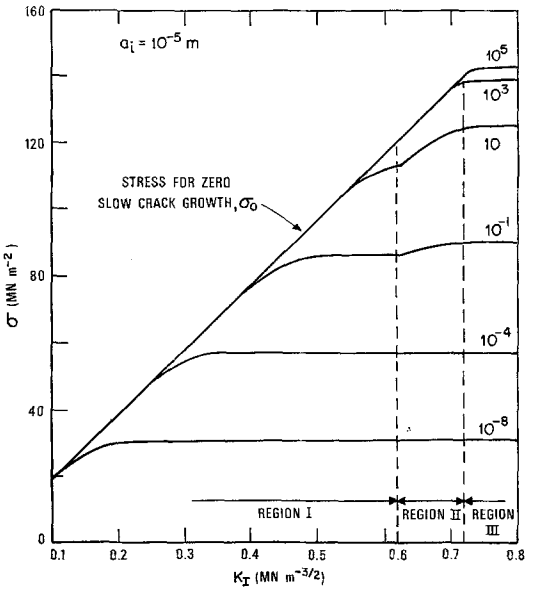

Figure 9 The relation between the stress intensity factor and the crack propagation stress for soda lime silicate glass specimens containing 10^{-5} m deep pre-existing flaws, tested in a 1% relative humidity environment: the number opposite each curve give the stress-rate in MN m^{-2} sec^{-1}.

(as shown in Fig. 10 and denoted region B); and the fracture stress above $\dot{\sigma}_s$ is easily obtained by equating σ_f to $(\sigma_{max})_3$, giving: $\sigma_f \propto \dot{\sigma}^{1/(n_3+1)}$ (denoted region C in Fig. 10).

The fracture stress between $\dot{\sigma}_c$ and $\dot{\sigma}_s$ is more difficult to evaluate and must be obtained by working through the details of the crack propagation behaviours in each region, using the parameters σ^* and K_I^*, as shown in Fig. 9. The resultant fracture stresses obtained are plotted in Fig. 10 (denoted region B'). It is interesting to note that these strengths are not very different from the strengths obtained if only regions I and III behaviours were considered (Fig. 10).

3. Empirical strength measurements

The empirical strength study was motivated by the need for extensive strength, stress-rate data on a system with a well-characterized three stage slow crack growth behaviour (to achieve an effective comparison of predicted and measured strengths). The system selected was soda lime glass in a 1% relative humidity environment, largely because good comparative fracture mechanics data were available [3], and also because reasonable flaw size consistency could be achieved using a standardized surface preparation procedure.

The strength tests were performed in four point flexure using specimens with an abraded surface. The test fixture was enclosed in a chamber and continuous streams of mixed dry and moist nitrogen gases were passed through the chamber during the tests to maintain the specimen environment at 1% relative humidity.

The analysis presented in the preceding section generated relations between stress-rate and fracture strength, that depend on the size of the pre-existing flaws, a_i. In order to compare measured and predicted strengths, therefore, we need either to determine a_i independently, or preferably, to ensure that comparisons are made at *constant* a_i. This latter approach can be effected, in principle, by performing a large number of strength measurements and using a proper sampling procedure to ensure a consistent flaw size distribution for each stress-rate condition. Consequently, fifty samples were allocated for each stress-rate condition; all samples (a total of 700 for 14 selected stress-rates) were prepared together from a single batch; then a random sampling approach was used to separate the specimens into groups of fifty.

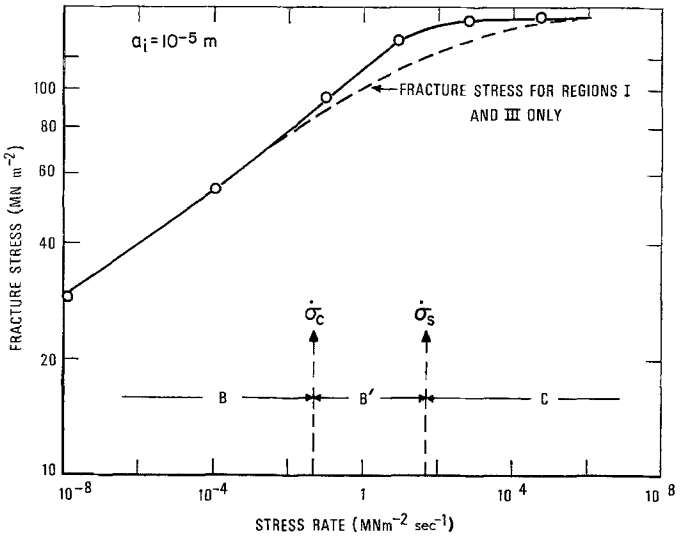

Figure 10 The predicted stress-rate dependence of the fracture strength of a soda lime silicate glass containing a 10^{-5} m deep initial flaw, tested in a 1% relative humidity environment.

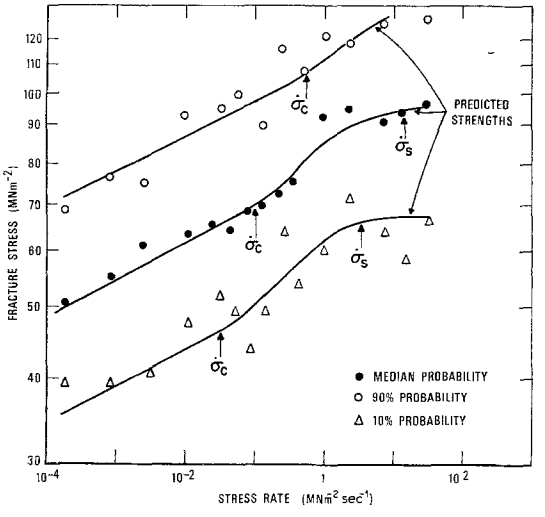

Figure 11 Flexural strength data obtained on a function of the stress-rate for abraded soda lime silicate glass: the solid lines are the strengths predicted from the fracture mechanics data.

A comparison of strengths at *constant* a_i can then be effected by plotting the median strengths (if the strength distributions are reasonably compatible) [8]. The results obtained are shown in Fig. 11. The general features described in the preceding section (and illustrated in Fig. 10) are evident, i.e. the three regions of behaviour, B, B′ and C are apparent. A more quantitative comparison can be made by first calculating an apparent value for a_i from the strength in region C^* (because, in this region, $K_I \approx K_{IC}$, the critical stress intensity factor); this gives $a_i = 2 \times 10^{-5}$ m. Inserting this value for a_i in the equations developed in the previous section enables the strength, stress-rate curve to be predicted from the fracture mechanics data (Fig. 8). The predicted strengths are plotted as the solid line in Fig. 11. A good correlation is apparent, showing that the slow crack growth parameters, n_1, A_1, V_b, n_3 and A_3 are essentially the same for the small flaws that control the strength behaviour and the macro-cracks used for fracture mechanics measurements.

A further critical comparison involves the examination of stress-rate effects at both a larger probability (smaller a_i) and at a smaller probability (larger a_i), because changes in a_i lead to distinctive trends in the predicted strength behaviour. Let us consider the probabilities; 0.9 and 0.1: the corresponding strength, stress-rate data are shown in Fig. 11. A distinct translation of region B′ toward higher stress-rates is apparent as the flaw size, a_i, is diminished. This is qualitatively consistent with the analytical predictions (Section 2.2.2). The complete strength predictions, evaluated in the manner described above, are shown as the full lines in Fig. 11. The

*No direct methods for evaluating a_i (for glass) have yet been devised.

good correlation with the measured strengths lends additional credence to the conclusion, noted above, that the micro and macro crack propagation parameters, for this material, are essentially equivalent.

4. Conclusions

An analysis has been presented which enables the strength, stress-rate relations for any system to be predicted, very simply, from the slow crack growth parameter, by identifying and evaluating several key quantities.

Slow crack growth data for soda lime silicate glass was used to illustrate the expected strength trends for a system that exhibits typical three stage slow crack growth behaviour. Three strength regimes were identified, but these were not as distinct as the regions of slow crack growth.

Finally, strength data obtained on soda lime silicate glass flexural specimens in a 1% RH environment were compared with the strength predicted from the fracture mechanics data. A good correlation was apparent suggesting that the conditions for the propagation of small pre-existing cracks and large macro-cracks are essentially the same for this material in a 1% RH environment.

References

1. R. J. CHARLES, *J. Appl. Phys.* **29** (1958) 1549.
2. A. G. EVANS, *Int. J. Fract.*, **10** (1974) 251.
3. S. M. WIEDERHORN, *J. Amer. Ceram. Soc.* **50** (1967) 407.
4. *Idem, Fracture Mechanics of Ceramics* **2** (1974) 613.
5. *Idem, Int. J. Fract. Mech.* **4** (1968) 171.
6. S. M. WIEDERHORN, H. JOHNSON, A. H. HEUER and A. M. DINESS, *J. Amer. Ceram. Soc.* **57** (1974) 336.
7. A. G. EVANS, *J. Mater. Sci.* **7** (1972) 1137.
8. A. G. EVANS and S. M. WIEDERHORN, NBSIR – 73-147, (March 1973); *Int. J. Fract.* **10** (1974) 379.

Received 31 May and accepted 22 July 1974.